Structural Responses of Secondary Lining of High-Speed Railway Tunnel Excavated in Loess Ground

Dingli Zhang[1], Qian Fang[1,*], Pengfei Li[1] and Louis Ngai Yuen Wong[2]

[1]School of Civil Engineering, Beijing Jiaotong University, Beijing 100044, China
[2]School of Civil and Environmental Engineering, Nanyang Technological University, Singapore 639798, Singapore

Abstract: To systematically study the mechanical properties and structural responses of the secondary lining for high-speed railway tunnels excavated in loess ground, on-site monitoring was performed to measure the contact pressure between the primary lining and secondary lining. It is found that the contact pressure reaches its first peak value when the tunnel formwork carriage is removed. The load acting on secondary lining is in the form of deformation pressure, which is different from the loose pressure prescribed in the China Tunnel Design Standard. The results obtained from this study enhance our understanding towards the mechanical characteristics of secondary lining for high-speed railway tunnels and are also beneficial to secondary lining design.

Key words: high-speed railway tunnel, secondary lining, on-site monitoring, safety factor.

1. INTRODUCTION

By the end of 2011, 9,900 railway tunnels with a total length of 7,100 km have been constructed for operation in China, 577 of which are high-speed railway tunnels with a total length of 810 km. During the construction of high-speed railway tunnels in China, the New Austrian Tunneling Method (NATM) has been widely adopted. This method is based on the principles established by Rabcewicz (1964a, b, 1965). Following this technique, a flexible, yet strong shotcrete is commonly adopted as primary lining, which is usually followed by bolting. After the deformations of the surrounding ground have become stabilized with the help of the primary lining, the cast-in-place secondary lining is installed in general practice.

According to the "Code for Design on Tunnel of Railway" (TB10003–2005), the primary lining is designed by empirical method in accordance with the surrounding ground classification, while the secondary lining is dimensioned by the hyperstatic reaction method (Duddeck and Erdmann 1985; Leca and Clough 1992; Oreste 2006). This method simulates the interaction between the support and surrounding rock through many independent "Winkler" type springs. The active loads (loose pressures), which are applied directly to the support structure, require to be estimated according to either the Code (TB10003–2005) or some technical documents (Bieniawski 1989; Singh *et al*. 1997; Barton 2002). However, due to the inherent uncertainties of the surrounding ground in nature, the active loads calculated are unreliable. Moreover, due to the existence of the primary lining, the loads acting on the secondary lining in general build up over time. Their magnitudes depend on the interaction between the primary and secondary linings, the durability of support structures, and the long-term effects. These entail the incompatibility of the design method of the secondary lining with its original design purpose.

In this paper, the structural responses of the secondary lining of a high-speed railway tunnel excavated in loess ground are studied. The radial contact pressures between the primary lining and secondary lining are first measured by using earth pressure cells. The structural responses of the secondary lining are then

*Corresponding author. Email address: qfang@bjtu.edu.cn. Tel: +86-10-51688115.

studied by the hyperstatic reaction method and the monitoring load method. Finally, the safety factors of the secondary lining obtained by the two methods are compared.

2. PROJECT OVERVIEW

The Hu Maling tunnel project in China involves building a single tube tunnel serving two-lane two-way high-speed railway traffic. One of its tunnel portals is shown in Figure 1. The total length of this tunnel is about 13,611 m (from DK68+626 to DK82+237). The maximum overburden thickness is about 295 m. It mainly tunnelled through late Quaternary loess. The ground qualities of the surrounding rock at the site are classified as Class IV and Class V according to the "Code for Design on Tunnel of Railway" (TB10003–2005). A simplified relationship between the surrounding ground quality and the Chinese classification BQ (basic quality) system, as well as the widely-used Q system is shown in Table 1 (Gan 2008).The tunnel cross-section dimensions adopted for Class IV and Class V ground conditions are shown in Figure 2.

Figure 1. North portal of the Hu Maling tunnel

3. INSTALLATION OF PRESSURE CELLS

Twenty one earth pressure cells were installed between the primary lining and the secondary lining in three cross-sections in the Hu Maling tunnel. The first section is located at DK68+973, of which the surrounding ground is classified as Class V. The second and third sections are located at DK69+210 and DK69+256 respectively, of which the surrounding ground is classified as Class IV. The minimum overburden depth of these three sections is 68 m. Therefore, all these three sections can be classified as deeply buried according to the Code (TB10003–2005). For each cross section, earth pressure cells were installed in seven positions: left knee, left waist, left shoulder, crown, right shoulder, right waist and right knee (Figure 3). The selected earth pressure cell is a

Table 1. Relationship between BQ system and Q system

	Class I (very good)	Class II (good)	Class III (fair)	Class IV (poor)	Class V (very poor)
BQ-value	>550	451–550	351–450	251–350	<250
Q-value	>40	10–40	4–10	1–4	<1

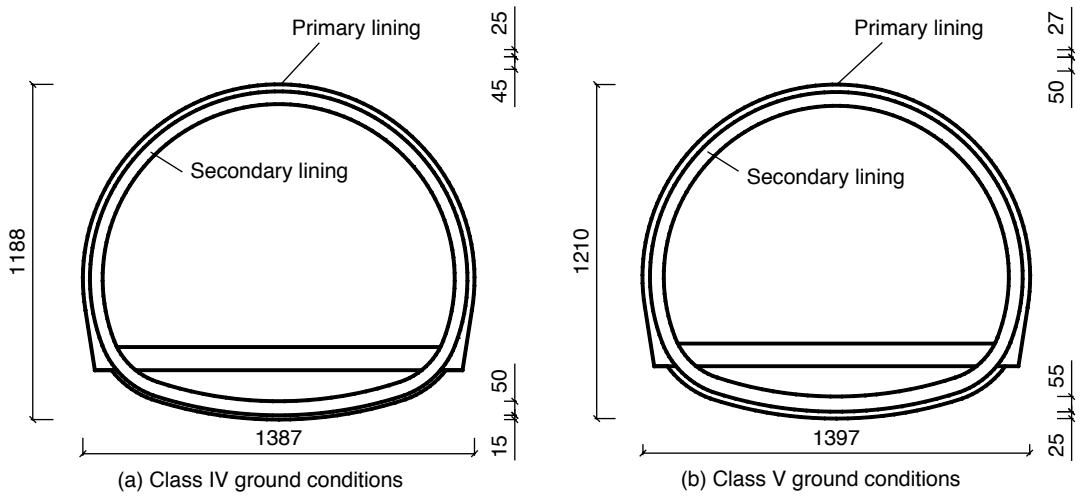

Figure 2. Tunnel cross-section (unit: mm)

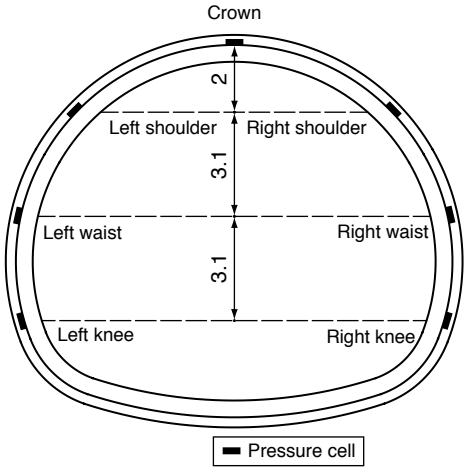

Figure 3. Layout of the measuring points (unit: m)

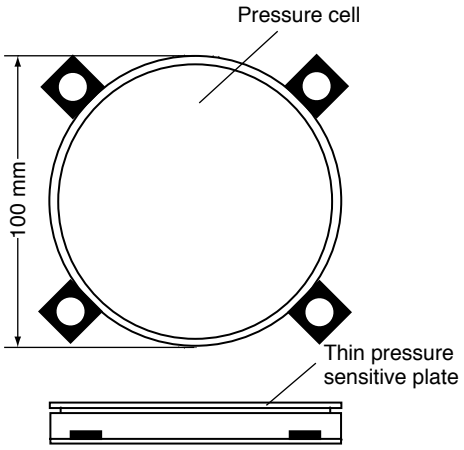

Figure 4. Earth pressure cell

kind of double-membrane cell, which is particularly designed for measuring soil pressures on structures. One of its plates, which bears against the external surface of the structure, is designed to have an adequate thickness to prevent flexure of the cell. The other plate, which is thinner, is designed to react with the soil pressure (Figure 4). At each position, one earth pressure cell was installed to measure the radial contact pressure between the primary lining and the secondary lining. The thick plate of the cell is placed against the primary lining and the thin plate is in contact with the secondary lining. Before the installation of each earth pressure cell, a particular area of the primary lining surface was first polished. Then the polished area was covered by a piece of non-woven fabric. After that the earth pressure cell was fixed on the primary lining above the non-woven fabric by a nail gun (Figure 5).

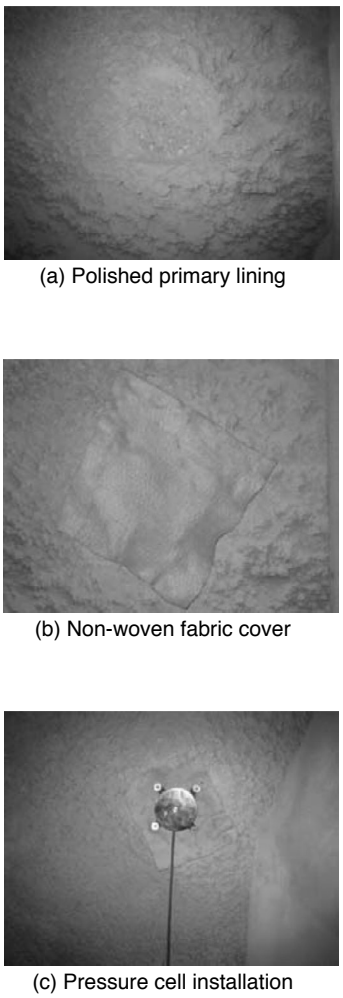

(a) Polished primary lining

(b) Non-woven fabric cover

(c) Pressure cell installation

Figure 5. Pressure cell installation procedure

4. MONITORING RESULTS

The measured earth pressure cell data of Section DK68+973, Section DK69+210 and Section DK69+256 are shown in Figure 6. The shaded region of each subfigure in Figure 6 displays a zoomed portion of the same set recorded in the early stage of monitoring. After reaching equilibrium, the pressure distributions of these three sections are obtained as shown in Figure 7. According to the monitoring results, the following observations are made:

(1) After the cast of the secondary lining concrete, the radial pressures between the primary lining and secondary lining increased immediately. They reached their first peak values when the tunnel formwork carriage was removed. From this time onwards, the measured pressures decreased dramatically until reaching their low points. Afterwards the pressures gradually increased. Several days later, the pressures became nearly stable;

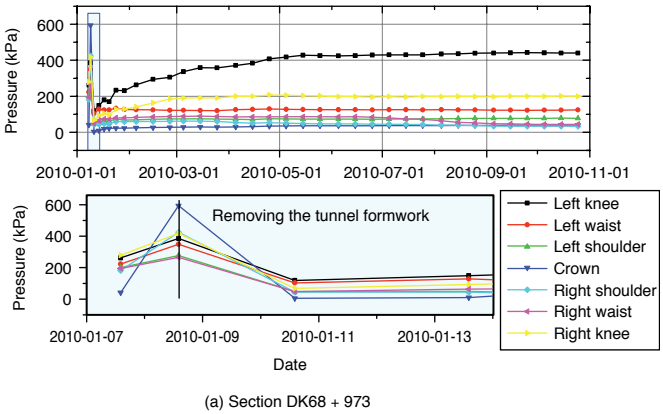

(a) Section DK68 + 973

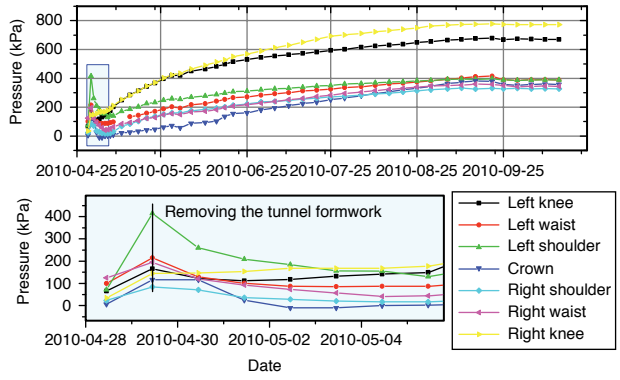

(b) Section DK69 + 210

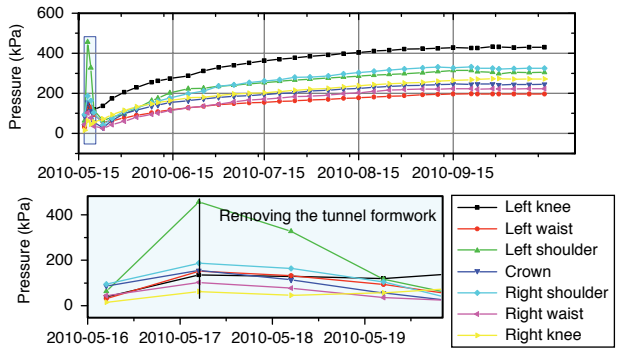

(c) Section DK69 + 256

Figure 6. Variation of measured contact pressures between the primary and secondary linings

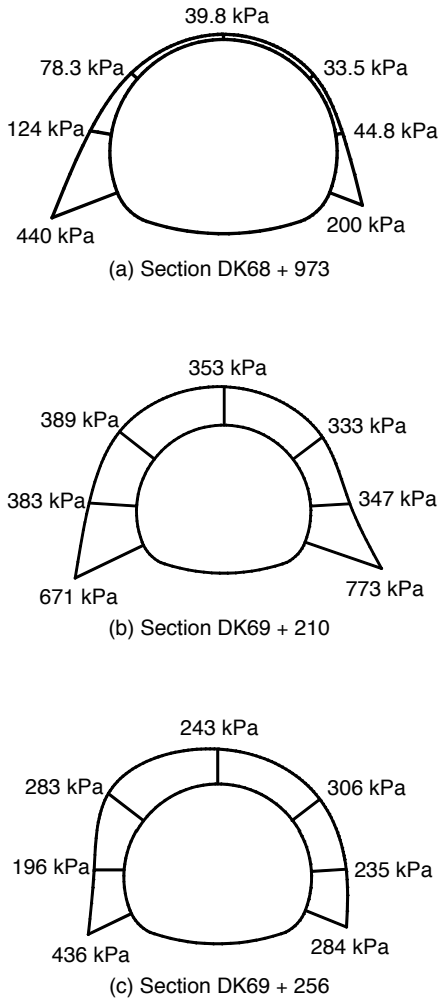

Figure 7. Contact pressure between the primary and secondary linings after reaching equilibrium

(2) Due to the differences associated with the construction logistics, the secondary lining of Section DK68+973 was not cast until the primary lining deformation became insignificant, while the secondary linings of Section DK69+210 and Section DK69+256 were cast only three days after the primary lining installation. Therefore, the measured pressures of Section DK68+973 were generally much smaller than the pressures measured at the same positions of the other two sections;

(3) The measured pressure distributions of the three sections varied greatly. In addition, they also differed significantly from the pressures calculated by the loose pressure theory.

5. STRUCTURAL ANALYSIS

The monitoring results of the radial contact pressures between the primary and secondary linings of the Hu Maling tunnel reveal that the loads transmitted to the secondary lining are in the form of "deformation pressure" instead of "loose pressure". In this section, a series of structural analyses of the secondary lining of the Hu Maling tunnel are performed. The structural responses of the secondary lining obtained by the traditional hyperstatic reaction method and the monitoring load method are also compared.

5.1. Structure Analysis Using the Hyperstatic Reaction Method

With reference to the "Code for Design on Tunnel of Railway" (TB10003–2005), the typical mechanical properties of Class IV and Class V surrounding ground are provided in Table 2. The loose body heights of Class IV and Class V surrounding ground under deeply buried conditions are 6.75 m and 13.54 m, respectively. The active pressure that acts on the roof of the secondary lining can be obtained by multiplying its weight by the loose body height. The mechanical parameters of the concrete of the secondary lining are shown in Table 3.

With the use of the commercial finite element program of MIDAS-GTS (MIDAS GTS 2009), the bending moments and normal forces along the secondary lining associated with the above two ground conditions can be calculated by the hyperstatic reaction method. Figure 8 shows the calculation results.

5.2. Structural Analysis Using the Monitoring Load Method

The monitoring loads that are applied on the secondary lining follow the patterns shown in Figure 7. In order to maintain the stability of the secondary lining, some normal springs are connected to the invert nodes. In addition, the node that represents the secondary lining crown and the node on the middle of the secondary lining invert are fixed horizontally to facilitate the structure to reach equilibrium. By using MIDAS-GTS, the structural responses are obtained as shown in Figure 9.

5.3. Comparisons of Structure Safety by the Two Methods

Although reinforcement is incorporated in the secondary lining of the Hu Maling tunnel, the safety factors are calculated for plain concrete secondary lining without considering the reinforcement. By neglecting the differences associated with the support reinforcement under different ground conditions, the safety factors can be obtained which allow for a more direct quantitative comparison. The comparison is performed on the safety factors obtained by the hyperstatic reaction method and the monitoring load method. According to the Code (TB10003–2005), for a rectangular concrete member under loading, if its eccentricity is less than or equal to 0.2 times of its thickness ($e_0 \le 0.2d$), the bearing capacity of the member is controlled by its compressive strength, i.e.

$$K \le \varphi \alpha R_c bd / N \tag{1}$$

where K denotes the safety factor of the concrete member; φ denotes the buckling coefficient, which is taken as 1 for a tunnel project; α denotes the acentric factor, which can be calculated by $\alpha = 1\text{-}1.5e_0/d$; R_c denotes the ultimate compressive strength of concrete; b denotes the height of the member; d denotes the thickness of the member; and N denotes the axial force of the member.

If the eccentricity of the concrete member is larger than 0.2 times of its thickness ($e_0 > 0.2d$), the bearing capacity of the member is controlled by its tensile strength, i.e.

$$K \le \varphi \frac{1.75 R_t bd}{N\left(\frac{6e_0}{d} - 1\right)} \tag{2}$$

where R_t denotes the ultimate tensile strength of concrete.

With the above formula, we can calculate the structural safety factors of the secondary lining. Because the length of the beam element is designated to be 0.5 m in the finite element calculations, totally 390 and 405 beam elements

Table 2. Mechanical parameters of surrounding ground

Ground class	Weight (kN/m^3)	Stiffness (MPa/m)	Lateral pressure coefficient
IV	22	350	0.15
V	18.5	150	0.3

Table 3. Mechanical parameters of concrete

Type	Weight (kN/m^3)	Elastic modulus (GPa)	Poisson's ratio	Compressive strength R_c (MPa)	Tensile strength R_t (MPa)
C30	23	31	0.2	22.5	2.2

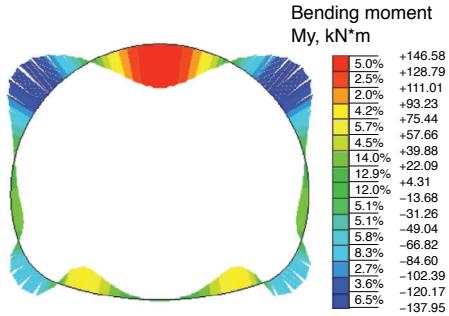

(a) Bending moments of class IV ground condition

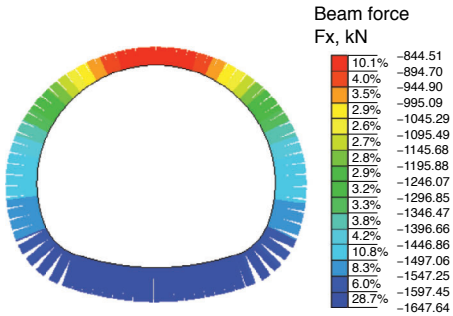

(b) Axial forces of class IV ground condition

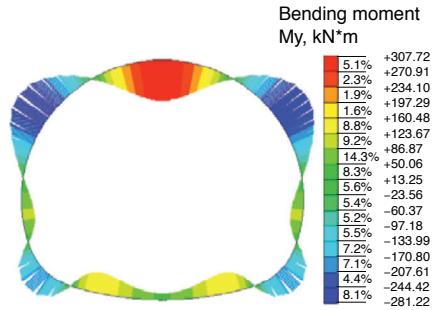

(c) Bending moments of class V ground condition

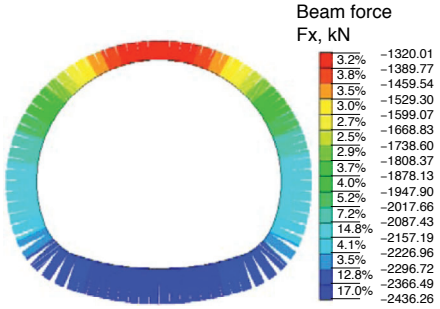

(d) Axial forces of class V ground condition

Figure 8. Secondary lining response under standard load

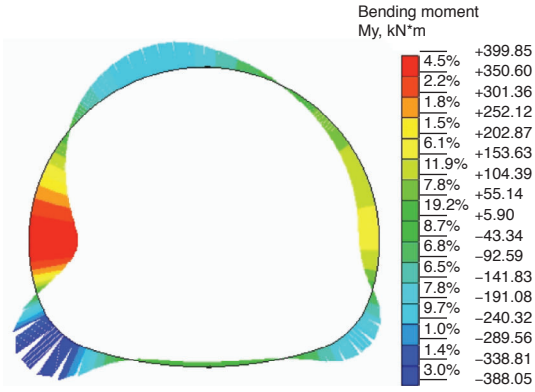

(a) Bending moments of section DK68 + 973

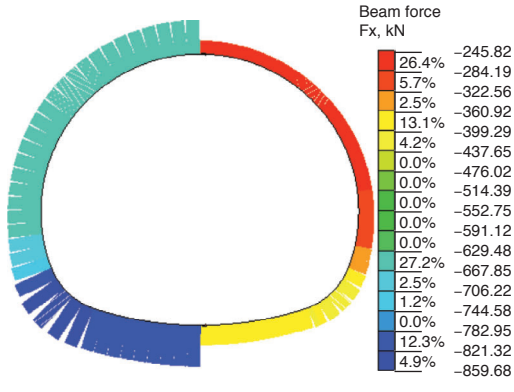

(b) Axial forces of section DK68 + 973

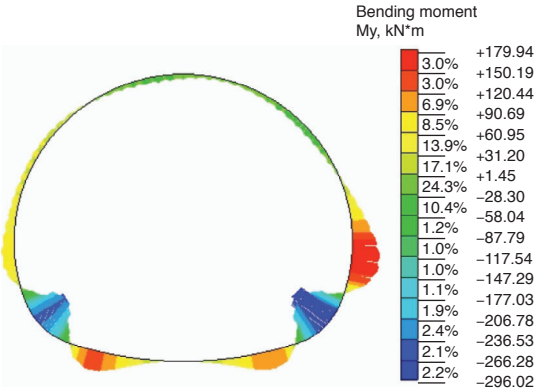

(c) Bending moments of section DK69 + 210

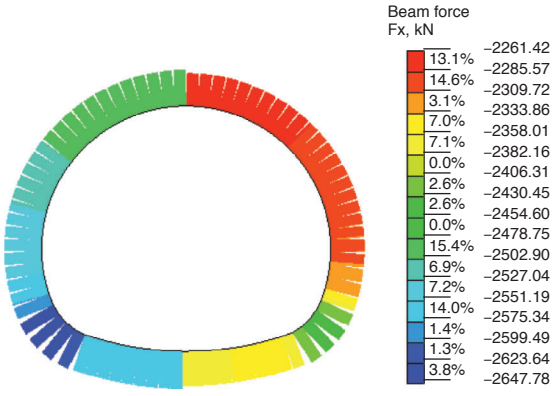

(d) Axial forces of section DK69 + 210

Figure 9. *Continued*

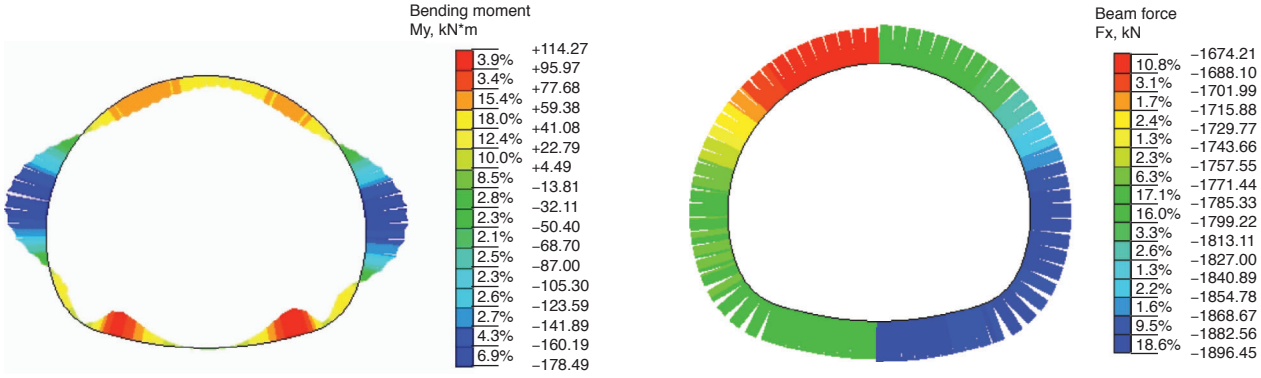

(e) Bending moments of section DK69 + 256

(f) Axial forces of section DK69 + 256

Figure 9. Secondary lining response under monitored load

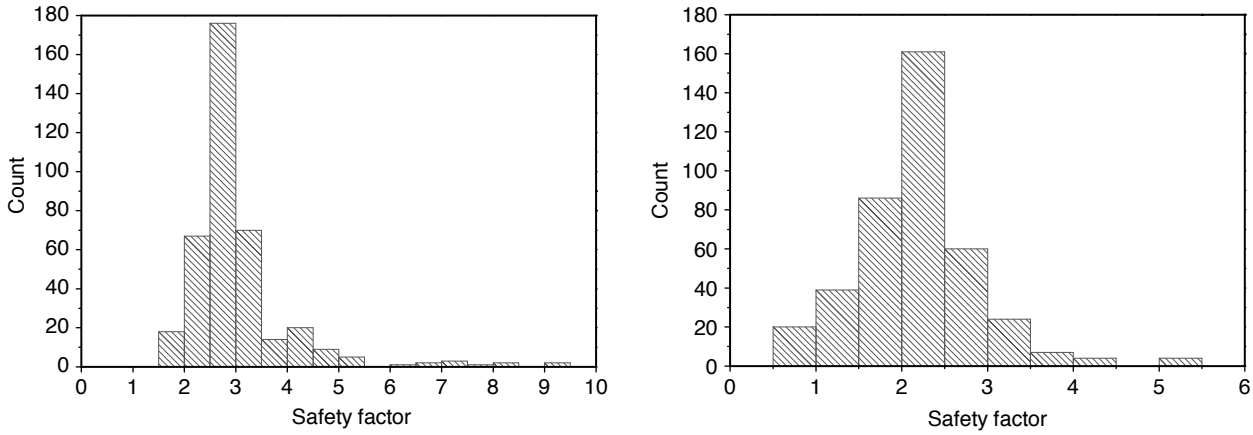

(a) Deeply buried class IV ground condition

(b) Deeply buried class V ground condition

Figure 10. Safety factors under standard load

are used in the Class IV and Class V ground conditions respectively. Histograms are plotted to help visualize the safety factor distribution of all the elements in a particular set of calculation. The results corresponding to the deeply buried Class IV and Class V ground conditions under the "standard load" are shown in Figure 10, while the results corresponding to the three sections under the "monitored load" are shown in Figure 11. In each histogram, the horizontal ordinate shows the distribution of the safety factors and the vertical ordinate shows the count of the beam element possessing a particular safety factor obtained from the calculation.

A comparison of the structural responses of the secondary lining under "standard load" and "monitored load" reveal some significant differences between these two conditions:

(1) Under the "standard load", the bending moment is the maximum and the axial force is the minimum on the tunnel crown (Figure 8). The element on the tunnel crown thus experiences the maximum tensile stress. The secondary lining commonly fails in tension due to the intrinsic weak tensile strength of concrete. Therefore, the most unfavorable position of the secondary lining is located on the tunnel crown. Under the "monitored load", however, the most unfavorable positions of the secondary lining are usually located in the other stress concentration positions, which are not usually on the tunnel crown;

(2) The distributions of the safety factors obtained by the "standard load" and the "monitored load" differ greatly. For Class IV ground condition, the safety factors obtained by the "standard load" mainly range from 1.5 to 5.5 [Figure 10(a)]. The tail of the histogram extends further to the right due to a relatively small number of counts of large safety factors.

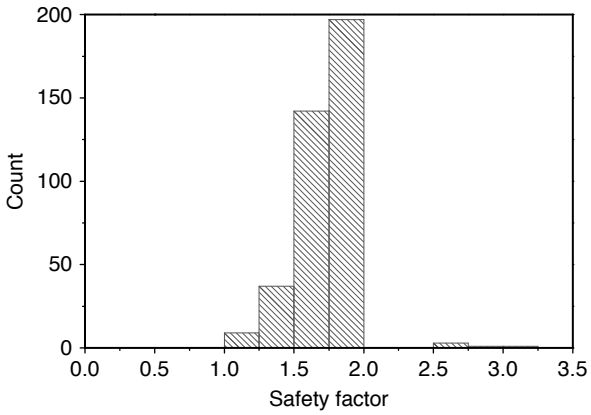

(a) Section DK 69 + 210 (class IV)

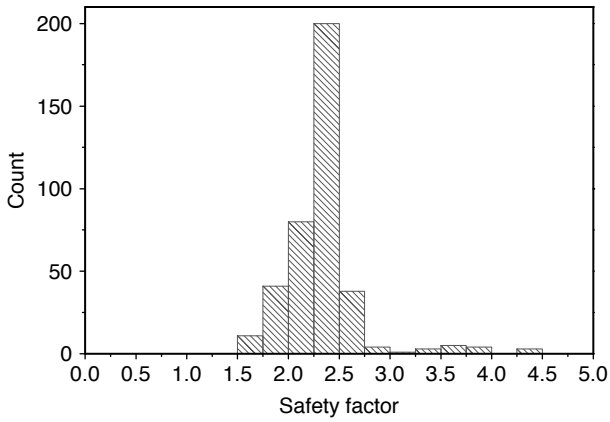

(b) Section DK 69 + 256 (class IV)

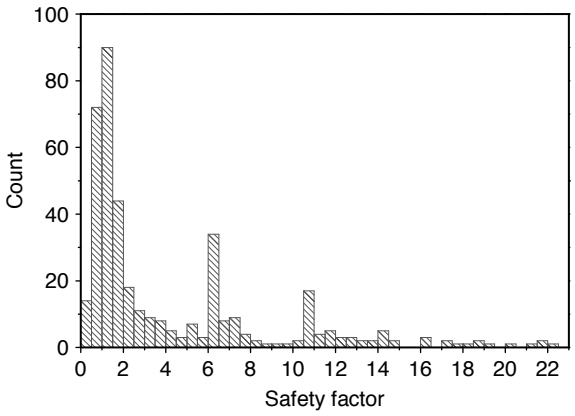

(c) Section DK 68 + 973 (class V)

Figure 11. Safety factors under monitored load

In contrast to the safety factors obtained by the "standard load" under Class IV ground condition, the safety factors obtained by the "monitored load" under Class IV ground conditions are more centralized [Figures 11(a), (b)]. However, for Class V ground conditions, the safety factors obtained by the "standard load" [Figure 10(b)] are more centralized than those obtained by "monitored load" [Figure 11(c)];

(3) For Class V ground conditions, a certain number of elements are found with a safety factor less than 1 based on both "standard load" and "monitored load" methods [Figures 10(b), 11(c)]. However, the structural analyses ignore the effect of the reinforcement. It is believed that with the contribution of the reinforcement, the structural safety can be ensured. This point of view has been validated by the successful and safe construction of the relevant sections;

(4) Although the measured loads of Section DK68+973 are considerably less than those measured in the other two sections, the minimum safety factor of Section DK68+973 is far less than those of the other two sections. This is due to the intensive stress concentrations present in the knees of the secondary lining at this section.

6. CONCLUSIONS

This paper studies the load-sharing effects on the secondary lining by on-site monitoring and numerical analysis. In summary, the following findings are obtained.

(1) The ground load applied to the secondary lining develops with time. The loads reach their first peak values when the tunnel formwork carriage is removed. At this time the strength of the concrete has not been sufficiently developed. Therefore, great caution should be taken in deciding when to remove the formwork. Moreover, the curing of the secondary lining concrete should be performed immediately and frequently after the removal of the formwork;

(2) For tunnelling in loess ground, the time effect of the load transmitted to the secondary lining is very significant. It may take several months for the stress in the secondary lining to reach equilibrium. This time effect requires a careful consideration of the consolidation and rheology effects in the loess tunnel design;

(3) The "deformation pressure" that is actually transmitted to the secondary lining differs significantly from the prescribed "loose pressure". The value of "deformation pressure" is closely related to the ground conditions and installation time of the secondary lining. Further

in-depth studies should be performed to estimate the loads acting on the secondary lining.

ACKNOWLEDGMENTS

The authors gratefully acknowledge the financial support by the Fundamental Research Funds for the Central Universities under Grant 2012JBM081, National Basic Research Program of China under Grant 2010CB732100 and the National Natural Science Foundation of China under Grant 51108020.

REFERENCES

Barton, N. (2002). "Some new Q-value correlations to assist in site characterisation and tunnel design", *International Journal of Rock Mechanics and Mining Sciences*, Vol. 39, No. 2, pp. 185–216.

Bieniawski, Z.T. (1989). *Engineering Rock Mass Classification*, John Wiley, New York.

Duddeck, H. and Erdmann, J. (1985). "On structure design models for tunnels in soft soil", *Underground Space*, Vol. 9, No. 5-6, pp. 246–259.

Leca, E. and Clough, W. (1992). "Preliminary design for NATM tunnel support in soil", *Journal of Geotechnical Engineering*, Vol. 118, No. 4, pp. 558–575.

MIDAS GTS (2009). *User Supports Web Page*. (http://www.midasuser.com/)

Oreste, P.P. (2007), "A numerical approach to the hyperstatic reaction method for the dimensioning of tunnel supports", *Tunnelling and Underground Space Technology*, Vol. 22, No. 2, pp. 185–205.

Rabcewicz, L. (1964a). "The new Austrian tunnelling method. Part I", *Water Power*, Vol. 16, No. 11, pp. 453–457.

Rabcewicz, L. (1964b). "The new Austrian tunnelling method. Part II", *Water Power*, Vol. 16, No. 12, pp. 511–515.

Rabcewicz, L. (1965). "The new Austrian tunnelling method. Part III", *Water Power*, Vol. 17, No. 1, pp. 19–24.

Singh, B., Goel, R.K., Jethwa, J.L. and Dube, A.K. (1997). "Support pressure assessment in arched underground openings through poor rock masses", *Engineering Geology*, Vol. 48, No. 1-2, pp. 59–81.

TB10003–2005 (2005). *Code for Design on Tunnel of Railway*, The Professional Standards Compilation Group of People's Republic of China, Beijing, China. (in Chinese)